d'Collection

Master's Thesis

Wavelet-Based EMG Sensing Interface for Pattern Recognition

Jonggyu Jang

Department of Electrical Engineering

Graduate School of UNIST

2019

Wavelet-Based EMG Sensing Interface
for Pattern Recognition

Jonggyu Jang

Department of Electrical Engineering
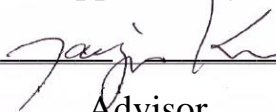
Graduate School of UNIST

Wavelet-Based EMG Sensing Interface

for Patter Recognition

A thesis/dissertation

submitted to the Graduate School of UNIST

in partial fulfillment of the

requirements for the degree of

Master of Science

Jonggyu Jang

12/11/2018
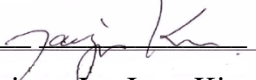
Approved by

_____

Advisor

Jae Joon Kim

Wavelet-Based EMG Sensing Interface
for Pattern Recognition

Jonggyu Jang

This certifies that the thesis of Jonggyu Jang is approved.

12/11/2018

signature

Advisor: Jae Joon Kim

signature

Yun Sik Lee: Thesis Committee Member #1

signature

Sung Phil Kim: Thesis Committee Member #2

Abstract

As interest in healthcare and smart devices has increased in recent years, the studies that are sensing and analyzing various bio signals, such as EMG, ECG, and EEG, have been growing. These studies and advances in smart devices have allowed human to increase access to their own physical information. With the physical information, human can diagnose himself or herself. These advances in technology will improve the quality of human life and provide solutions in various fields.

The convergence of information and communication technologies has led to the fourth industrial revolution and the development of artificial intelligence, big data and the Internet of Things(IoT) by increasing computing power has led to various data analysis using machine learning. Various fields are moving toward the next level using machine learning, and this trend is also happening in the healthcare field. The era of self-diagnosis begins when medical knowledge, which had previously been entrusted to doctors is passed directly to consumers through big data and machine learning. Thanks to these developments, the healthcare interface, such as front-end integrated chip, is also working to leverage machine learning to deliver various solutions to consumers.

Existing papers related to bio signals are focused on reducing power consumption, allowing long-term monitoring or reducing various noise. This paper provides an idea to extend the scope of data processes through machine learning while maintaining existing trends. Wavelet transform is implemented as a circuit to reduce computing power and eliminate specific frequency range including noise and motion artifact. The data from the chip is transmitted to external device (MATLAB) by wireless communication (Bluetooth) to be analyzed by machine learning. This paper present wavelet-based EMG sensing interface which includes front-end amplifier, wavelet filters, Analog to digital converter and Microcontroller. The main idea of the paper is front-end amplifiers which reduce a noise and motion artifact, wavelet filters that decompose the input signal for wavelet transform and machine learning for gesture recognition.

Contents

List of Figures

List of Tables

Abbreviations

ADC: Analog-to-Digital Converter

BW: Bandwidth

CCIA: Capacitively Coupled Instrumentation Amplifier

CWT: Continuous Wavelet Transform

ΔΣ: Delta-Sigma

DSP: Digital Signal Processing

DWT: Discrete Wavelet Transform

ECG: Electrocardiography

EMG: Electromyography

EOG: Electrooculography

LNA: Low Noise amplifier

LPF: Low Pass Filter

LSB: Least significant bit

MCU: Microcontroller

MSB: Most significant bit

MUX: Multiplexer

PPG: Photoplethysmography

PGA: Programmable Gain Amplifier

ROIC: Readout Integrated Circuit

RMS: Root Mean Square

Chapter 1

Introduction

This chapter describes the basic information that should be mentioned before explaining the implementations in this paper. First, the information of bio signals will be described. Second, some kinds of data processes that are used in bio signal analysis will be explained.

1.1 Bio signals in healthcare
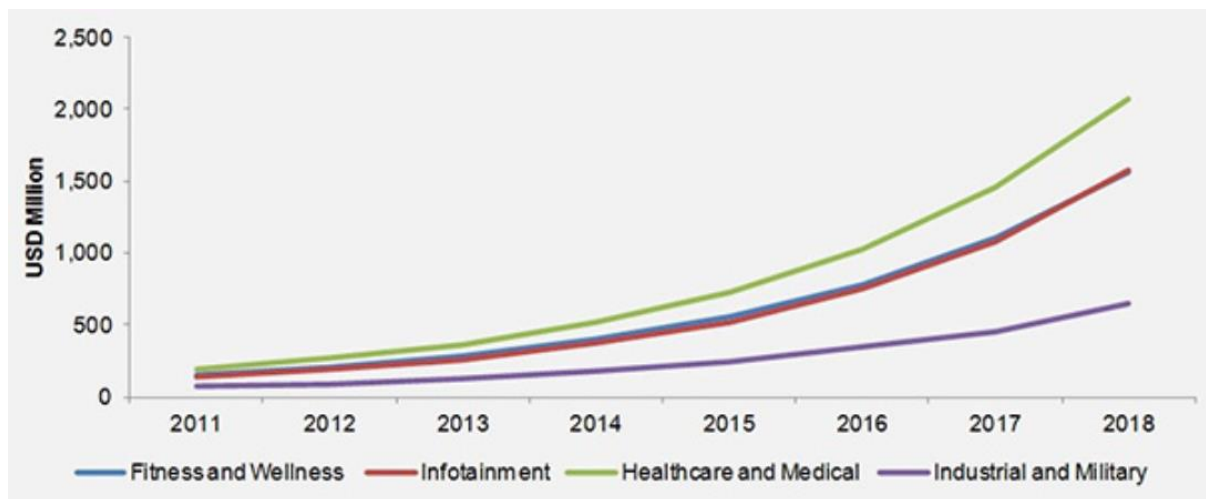
Fig. 1 Worldwide wearable electronics market growth from 2011 to 2018.

Recently, with the fourth industrial revolution, information and communication technologies (ICT) are developed rapidly, and it is followed by artificial intelligence(AI), quantum computing, biotechnology, robotics, the internet of things(IOT), 3D printing and fully autonomous vehicles [1]. This revolution leads people to focus on their life. With this desire, many companies are jumped to the wearable and smart device industrial to improve the quality of consumers' life. Fig. 1 shows market growth trends of wearable technology from 2011 to 2018. Before the 4th industrial revolution, wearable technology is used only in the industrial area. However, wearable technologies in healthcare and medical, fitness and wellness, infotainment areas are rapidly grown since the consumer's desire that is mentioned before [2]. With the growth of healthcare and the medical wearable device market, the interfaces that analyze a bio signals have been researched recently.

- **EEG : Electroencephalogram (brain)**
- **EOG : Electrooculogram (eyes)**
- **ECG : Electrocardiogram (heart)**
- **PPG : Photoplethysmography (skin)**
- **EMG : Electromyogram (muscle)**

(a)   **(b)**
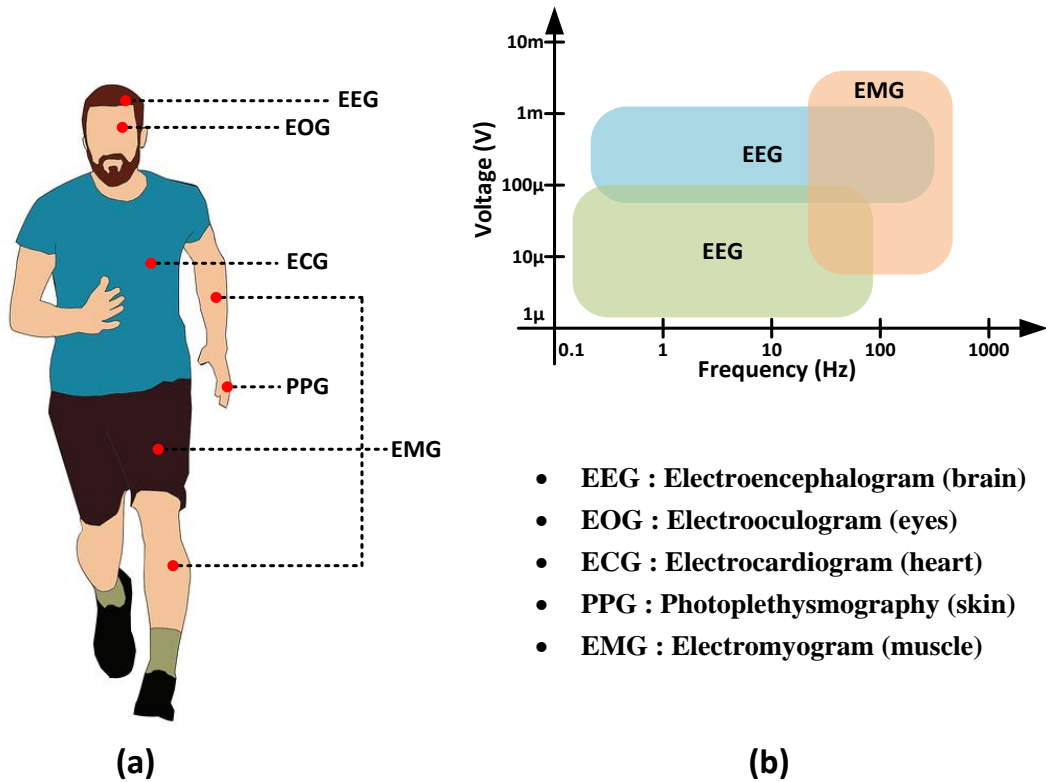
Fig. 2 (a) Bio signals in a human body, (b) Voltage ranges and bandwidths of signals.

Fig. 2 shows bio signals that are usually used in wearable devices. Each bio signal occurs at each part of the body. From the head of Fig. 2(a), Electroencephalography (EOG) is occurred from a brain. EEG is usually used to record electrical activity of the brain. The application of EEG is to diagnose of encephalopathy and anesthesia [3]. Electrooculography (EOG) occurs from eyes. EOG is usually measured movement of eyes [4]. Electrocardiography (ECG) occurs from heart. ECG is measured in time domain and used to detect any cardiac problems [5]. Photoplethysmography (PPG) is the signal that shows the changes in light absorption of the skin. To obtain a PPG, pulse oximeter is used to illuminate the skin. The application of PPG is monitoring breathing, hypovolemia, and other circulatory conditions [6]. Electromyography (EMG) occurs from muscle on the whole body. EMG is usually used in robot arm, artificial limb, and muscle pain since it shows the activation level of muscle and medical abnormalities [7]. Fig. 2(b) shows voltage range and frequency range of each bio signal. Every bio signals have their own properties in voltage domain and frequency domain. With these properties, the process that analyzes the bio signal is developed and used to diagnose and research many diseases and physical disorders.

Sensing those bio signals is not easy since there are many obstacles. First, as shown in Fig. 2(b), the bio signals have small amplitude of voltage thus the bio signal need to be amplified with large gain.

However, not only the signal but also the noise is amplified. The noises are generated from many routes. Most critical noise is from electrode which is attached to the body. The resistances on the skin are different due to how well the electrodes are attached. The difference resistance in the input stage results offset from the output stage. When the part of the body which the electrodes are attached on has movement, this noise is usually generated. It is called motion artifact. To measure the bio signal without motion artifact, the amplifiers in sensing interface, specifically in the integrated circuit, need additional circuit for reducing a noise.

1.2 Data process of Bio signal
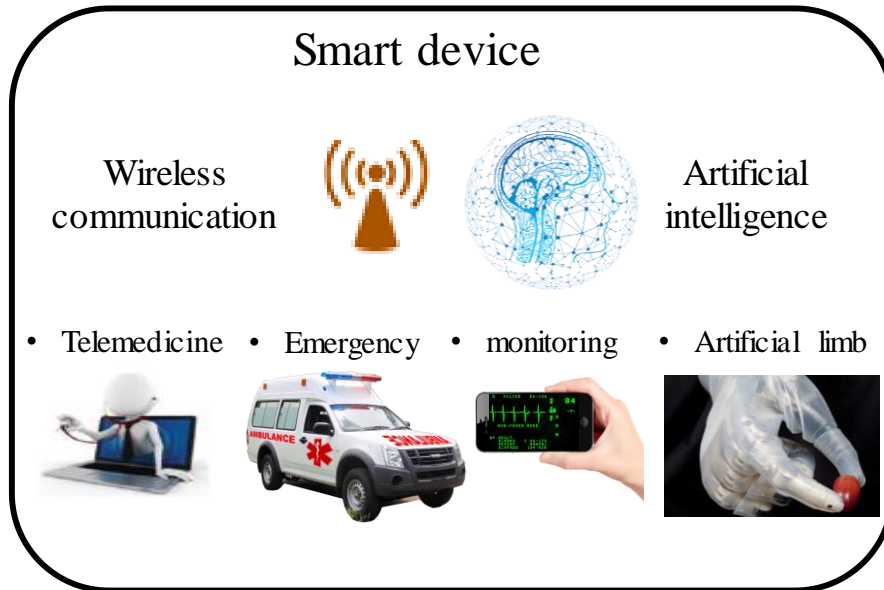
Fig. 3 Smart device interface with bio signals.

Fig. 3 shows the interface of smart devices with bio signals. With the 4th industrial revolution, ICT and artificial intelligence have been developed. The development of ICT leads electronics to transmit an information with faster wireless communication. faster transmission increases the amount of data that can be analyzed. With the fast and large amount of data, the applications of smart device are expanded. At the beginning of the smart device, smart device just measured the bio signal and transmitted the information for just monitoring. In these days, the telemedicine and self-diagnose becomes possible since the analysis of bio signals can detect any kind of medical abnormalities and the precise analysis can be used to control robot arms or artificial limb. Fig. 4 shows smart devices in these days. Fig. 4(a) is smart watch that uses the PPG to measure oxygen saturation. Fig. 4(b) is smart clothes that can measure ECG and EMG to detect physical abnormality. Fig. 4(c) is EEG cap that is used to analyze any disorder or disease of the brain.

(a) Smart watch   (b) Smart clothes   (c) EEG cap

Fig. 4 smart devices using bio signals.

(a) Fourier Transform   (b) Wavelet Transform

Fig. 5 Time-frequency tile allocation of the transforms:
(a) Fourier transform, (b) Wavelet Transform

Fig. 5 shows time-frequency tile allocation of Fourier transform and Wavelet Transform [8]. Fourier transform is well known as frequency domain analysis, but it has several constraints to analyze in time domain. As shown in Fig. 5(a), Fourier transform doesn't have information in time domain. If the frequency of the signal changes at a certain time, Fourier transform can't tell when a certain change occurs. Though the short time Fourier trans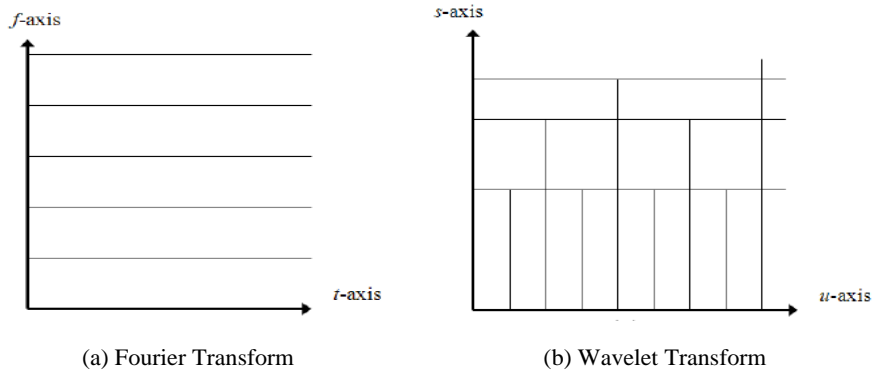form that implements Fourier transform in short time to find time information, it's frequency resolution depends on the time resolution. It means how short the time that the data is sampled for decides the frequency resolution. However, Wavelet transform overcomes these issues with equation 1.1

$$ W f(s, u) = \int_{-\infty}^{\infty} f(t) \frac{1}{\sqrt{s}} \psi^* \left(\frac{t-u}{s} \right) dt \qquad (1.1) $$

Since the mother wavelet function ψ^* is modulated by scale factor s, low frequency components are transformed with large s while high frequency components are transformed with small s. it means the wavelet transform can zoom in a certain frequency range with scale factor s. with this property, the wavelet transform has both time and frequency information.

(a) Time vs Voltage   (b) Voltage vs Frequency   (c) Time vs Frequency
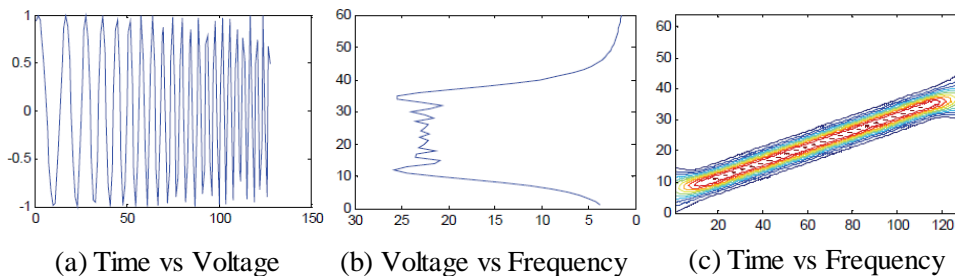
Fig. 6 Example of the wavelet transform

Fig. 6 shows the example of the wavelet transform [9]. Fig. 6(a) shows the signal that is not stationary in time domain. The voltage and frequency of the signal is changing with time. Fig. 6(b) is the description of the signal without time information. However, Fig. 6(c) shows the time-frequency

5

description. it shows time in x-axis, frequency in y-axis and magnitude in z-axis. With magnitude information, the signal can be analyzed in both time and frequency domain.

   This paper proposes EMG sensing interface with denoising circuit and filters to analyze the EMG efficiently. Overall system includes front-end amplifiers, wavelet filters, 12bit successive approximation analog to digital (SAR-ADC), and Microcontroller (MCU). The front-end amplifiers have special circuit to reduce the motion artifact and to be controlled by MCU. The wavelet filters consist of several Low-pass filters (LPF) which can decomposed the signal. The chip is implemented in 0.18 μm CMOS process. The result of the chip is processed by MATLAB machine learning thus the gesture of fingers can be recognized in frequency domain.

Chapter 2

Front-end circuit for Bio signal sensing

There are some techniques in front-end readout integrated circuit(ROIC) for sensing a bio signal. Front-end ROICs mean integrated circuit which is designed to sense and control signals in a chip. Front-end ROICs include some kinds of amplifiers to sense a specific signal. To sense a specific bio signal, amplifiers that are used in front-end ROICs need specific gain and bandwidth because bio signals have their own range of frequency and range of voltage. In this chapter, some circuit techniques that are used to sense bio signals and reduce noise and offset in a chip are explained.

2.1 Front-end circuit
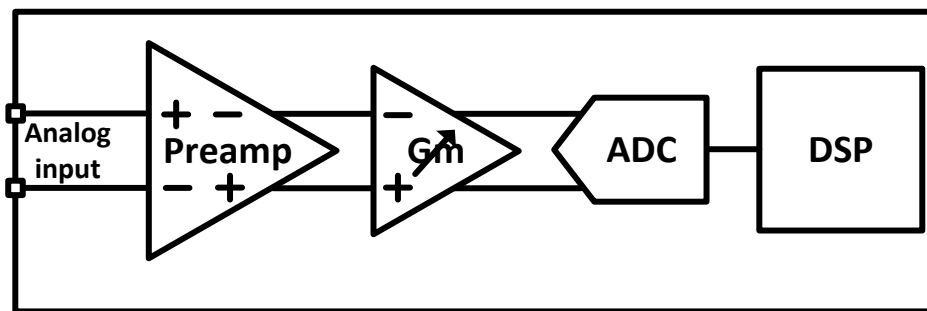
Fig. 7 Simple structure of bio signal sensing system.

Fig. 7 shows the simplest structure of bio signal sensing system. The system include preamp, programmable gain amplifier(PGA), analog-to-digital convertor and digital signal processing circuit. Since bio signals have their own range of voltage and range of frequency, preamp must have a specific bandwidth and gain according to the bio signal which is sensed. Also, preamp must mitigate a noise. PGA supports preamp by provide more gain. After analog signal processing, analog signals are converted to digital data by Analog to Digital converter(ADC). then digital data are analyzed with digital signal processing(DSP).

In bio signal sensing and monitoring, the motion artifact is important because most bio signal sensing devices operate with electrode that direct contact with human skin. When the subject has physical movements while the bio signal is sensing, it causes unstable contact between skin and electrodes. Unstable contact changes the contact impedance then result fluctuations in transient signal. Therefore, there have been recent works to mitigate a motion artifact.

2.1.1 Chopper stabilization

(a)

(b)
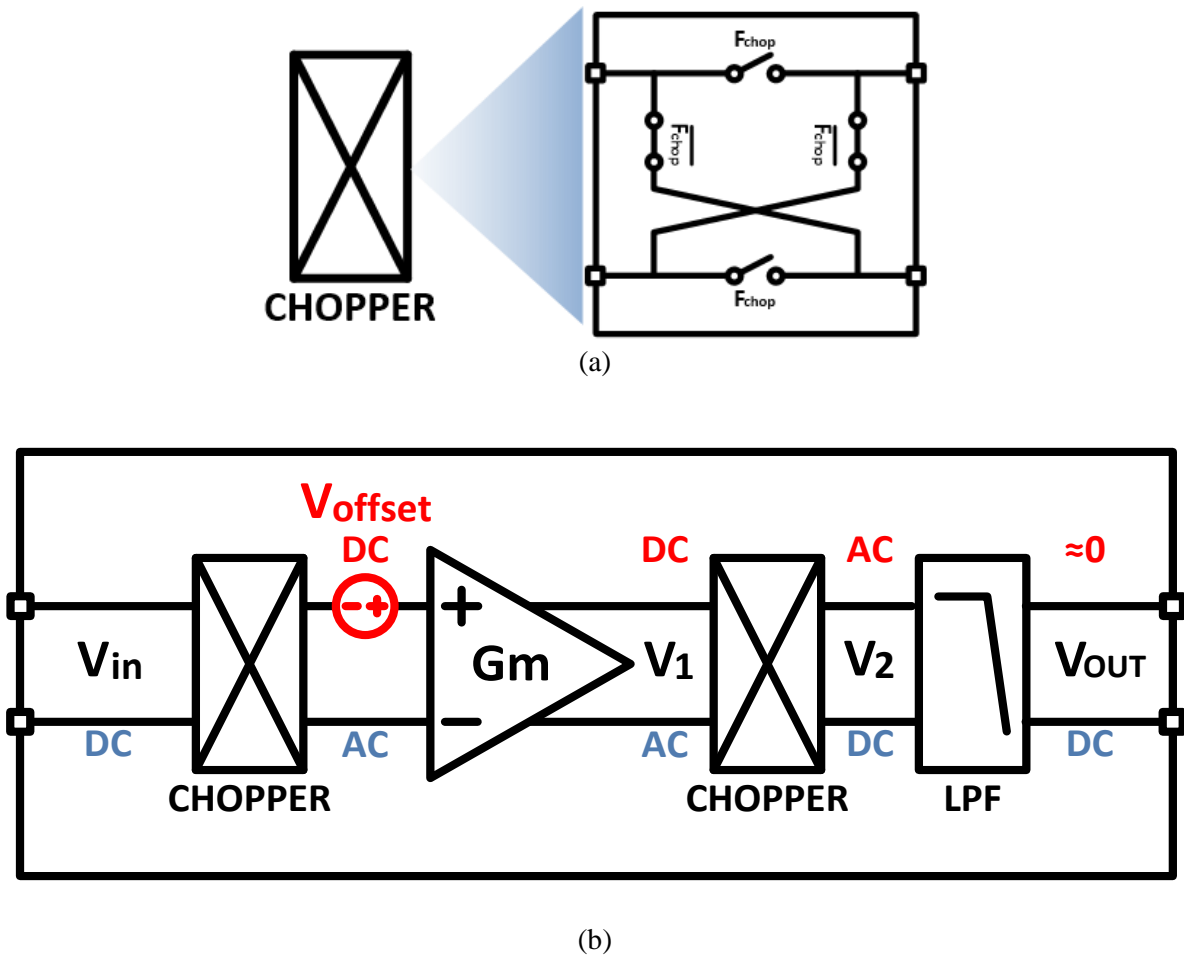
Fig. 8 Block diagram of chopping stabilization.

Noise in a chip is crucial to the quality of bio signal sensing as well as motion artifact. To reduce the noise, specially input referred noise, in a chip, chopping stabilization is generally used in these days. Fig. 8 shows the operation of chopping stabilization. There are two chopper blocks that modulate and demodulate the signal. The chopper consists of four switches. At each clock, forward path and crossed path are connected. After the first chopper, the signal is modulated from DC to AC. AC signal is amplified by the amplifier and demodulated from AC to DC by the second chopper. However, offset voltage that occurs at the amplifier is not modulated from the first chopper. Since offset is DC signal, offset is modulated from DC to AC by the second chopper. As a result, the offset becomes AC signal which frequency is high. To remove the offset that is high frequency component, a low pass filter(LPF) is used after second chopper.

8
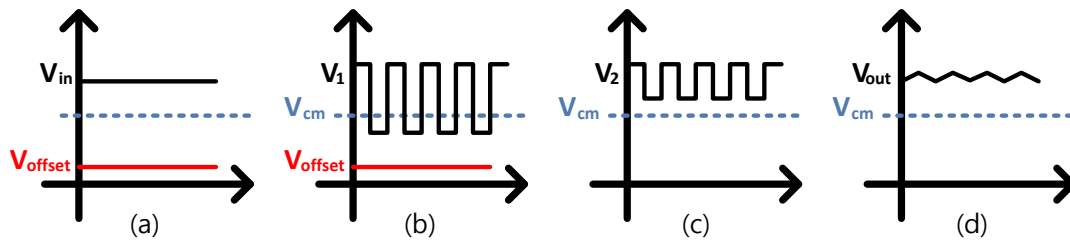
Fig. 9 The waveform of chopping stabilization in time domain.
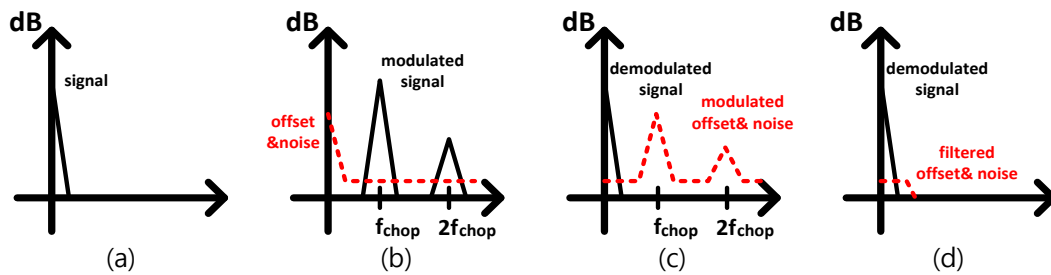
Fig. 10 Chopping stabilization in frequency domain.

Fig. 9 shows the waveform of chopping stabilization in time domain. The input analog signal V_{in} is modulated by the first chopper and amplified to V_1. In Fig. 9(b), DC offset that occurs in an amplifier makes the center voltage of V_1 shifted by the value of offset voltage. It means the center voltage of V_1 is not V_{cm}. This DC offset voltage is modulated by the second chopper. However, the input signal that is modulated from DC to AC by the first chopper is demodulated from AC to DC by the second chopper in Fig. 9(c). after that high frequency component is removed using LPF. As a result, in Fig. 9(d), DC input signal passes through the chopper system without any mitigation and DC offset and noise which have a high frequency component are eliminated. Fig. 10 shows chopping stabilization in frequency domain. Since the chopper modulates its input signal, the center frequency of the input signal becomes chopping frequency. The offset and noise are only modulated with chopping frequency then they are eliminated by low pass filtering. The instrumentation amplifier that uses a chopper stabilization is called the capacitively coupled instrumentation amplifier.

2.1.2 DC Servo Loop (DSL)

Main issues in bio signals are high common-mode interference and the differential electrode offset that is caused by the differential body potentials at each electrode. These issues result a small DC offset at the input stage of an amplifier. Most amplifiers for the bio signal have high gain because bio signals have low amplitude of voltage. The DC offset at the input stage of amplifiers is amplified with high gain then it results saturation at the output stage. For this reason, DC servo loop is necessary to remove DC offset.
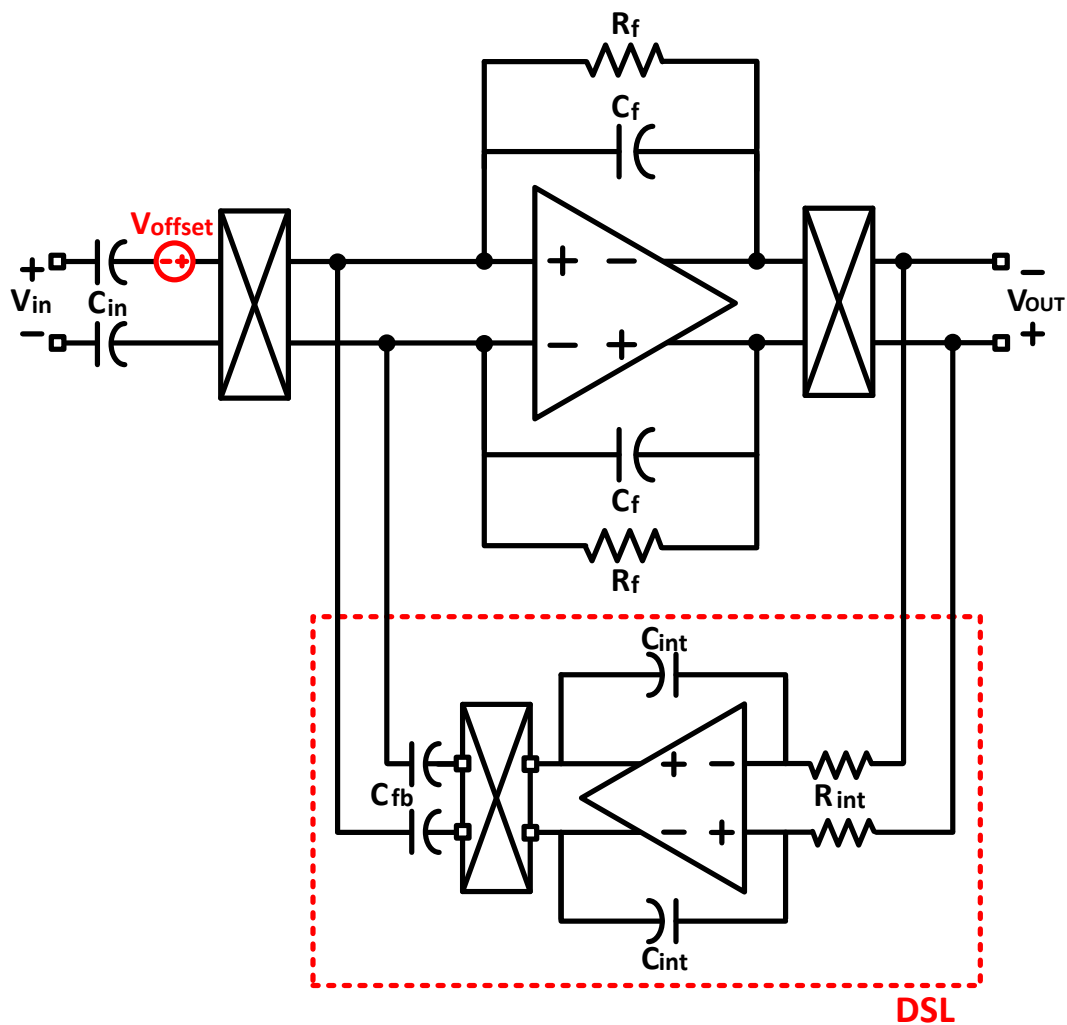
Fig. 11 Schematic of DC Servo Loop.

Fig. 11 shows schematic of the DSL. The operation of the DSL is as follows. DC offset voltage that occurs at the input stage of the capacitively coupled instrumentation amplifier (CCIA) is amplified CCIA then is integrated by the fully differential integrator. Since the input of CCIA is modulated, the

integrated offset is modulated to the high frequency by chopper and is negatively fed back to the input stage of CCIA. The transfer function without DSL and the transfer function with DSL is shown as Equation (2.1) and (2.2), respectively:

$$\frac{V_{out}(s)}{V_{in}(s)} = -\frac{sR_fC_{in}}{1+sR_fC_f} \tag{2.1}$$

$$\frac{V_{out}(s)}{V_{in}(s)} = -\frac{s^2R_fR_{int}C_{int}C_{fb}C_{in}}{(1+sR_fC_f)(sR_{int}C_{int}C_{fb}-C_f)} \tag{2.2}$$

In comparison with (2.1) and (2.2), the transfer function with DSL has the additional pole which frequency is $C_f/(C_fR_{int}C_{int})$. As a result, CCIA becomes a second order High pass filter by DSL then DC offset that has low frequency component is removed.

2.1.3 Ripple Reduction Loop (RRL)
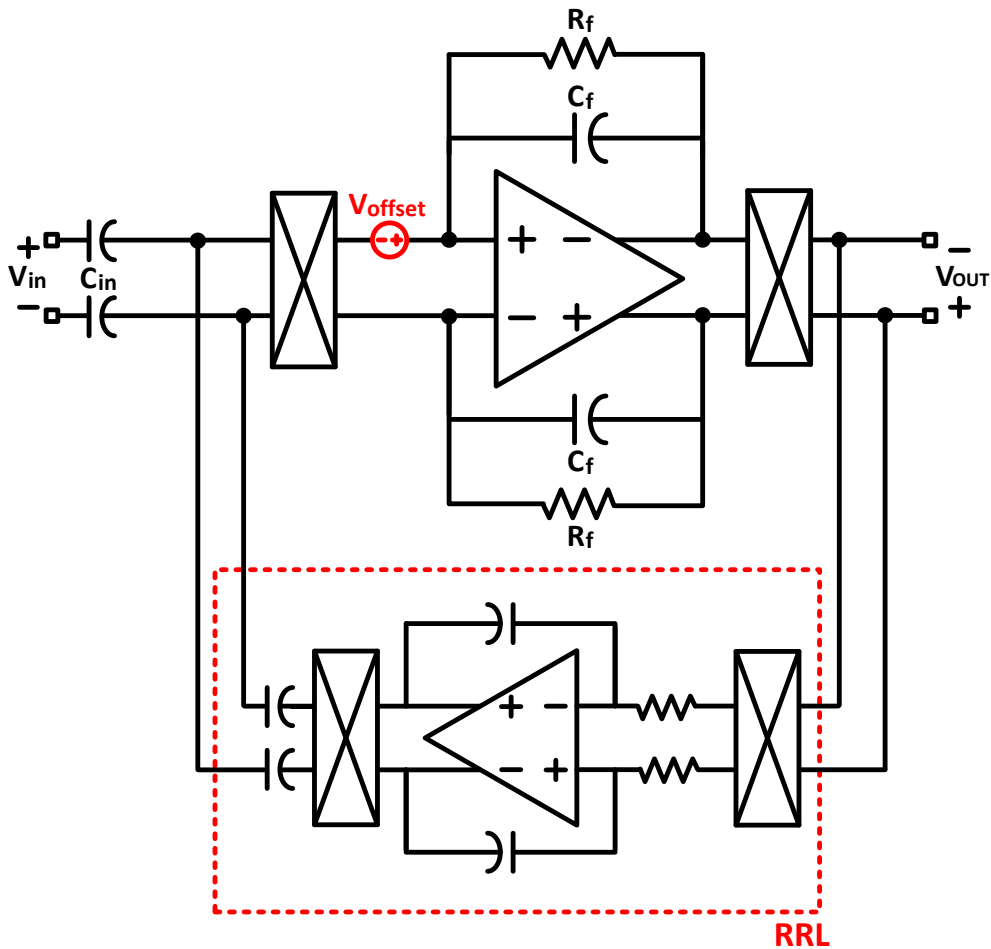
Fig. 12 Schematic of ripple reduction loop

The offset that is caused by the input transistor mismatch in CCIA is modulated by the second chopper then becomes a ripple at the output stage. Fig. 12 shows the schematic of the RRL. The ripple that is induced by the second chopper is demodulated to DC offset by the input chopper of the RRL. As same as DSL, offset is integrated by the following differential integrator. After integration, integrated offset is modulated by the output chopper of the RRL and is negatively fed back to input stage of CCIA. The difference between DSL and RRL is a position that the output of loop is fed back to. Since the output of RRL is modulated and demodulated by two choppers, it is fed back to before the first chopper of CCIA. However, the output of DSL is only modulated by one chopper then it is fed back to after the first chopper of CCIA.

2.2 Data process

The analog bio signal is measured in front-end amplifier with denoising circuit then converted to digital data in ADC. The digitized bio signal is just a raw data which have only voltage information. To extract the meaningful information, the data process is necessary that is implemented outside of integrated chip. Section 2.2 will focus on methods of data processing for bio signals and explain the reason that wavelet transform is used for the EMG sensing.

2.2.1 Data processing for bio signal

Currently, as the amount of data transmitted through the fourth industrial revolution increases exponentially, the way to analyze a bio signal has also been developed. Before the revolution, the only amplitude in time domain is useful information and it is difficult to analyze the bio signal in real-time. The easiest way to monitor a bio signal is envelop detecting. It follows an envelope of the input signal then gives an amplitude information in time domain. Its application is detecting a specific time when the peak occurs. This application is suitable for sensing the signal such as ECG that has a distinctive waveform. By finding peak time, it can calculate a heart rate and relative blood pressure with PPG. However, the main drawback is that envelop detecting can't find any frequency information.

To analyze a bio signal such as EMG and EEG that are identified by frequency instead of specific waveforms, Fourier transform is most commonly used method. As mentioned in section 1.2, Fourier transform converts an amplitude in time domain to the amplitude in frequency domain. However, Fourier transform isn't suitable for non-stationary signal. In other words, Fourier transform can't find the time when a signal with a specific frequency occurs. To overcome this, short-time Fourier transform is used but it is not possible for detailed analysis because it converts with a uniform sampling period. For this reason, Fourier transform is not the best solution for bio signal analysis.

2.2.2 Wavelet transform for bio signal

Bio signals are sparse signals that have a few number of meaningful elements and the other elements don't have any information. Also, bio signals have very low frequency and they are non-stationary signals whose frequencies vary with time. In other words, the bio signal is usually constant and sometimes occurs when the specific gesture or condition of body changes. Because of these features, time and frequency information is required to analyze a bio signal properly. For this reason, Wavelet transform is good for analyzing sparse and non-stationary signal rather than Fourier transform. As mentioned in section 1.2, unlike Fourier transform, wavelet transform has both frequency and time information. Wavelet transform has a filter bank that decomposes the raw signal then generates coefficients. Noise reduction and data compression that are the main application of wavelet transform are performed by processing these coefficients [12].
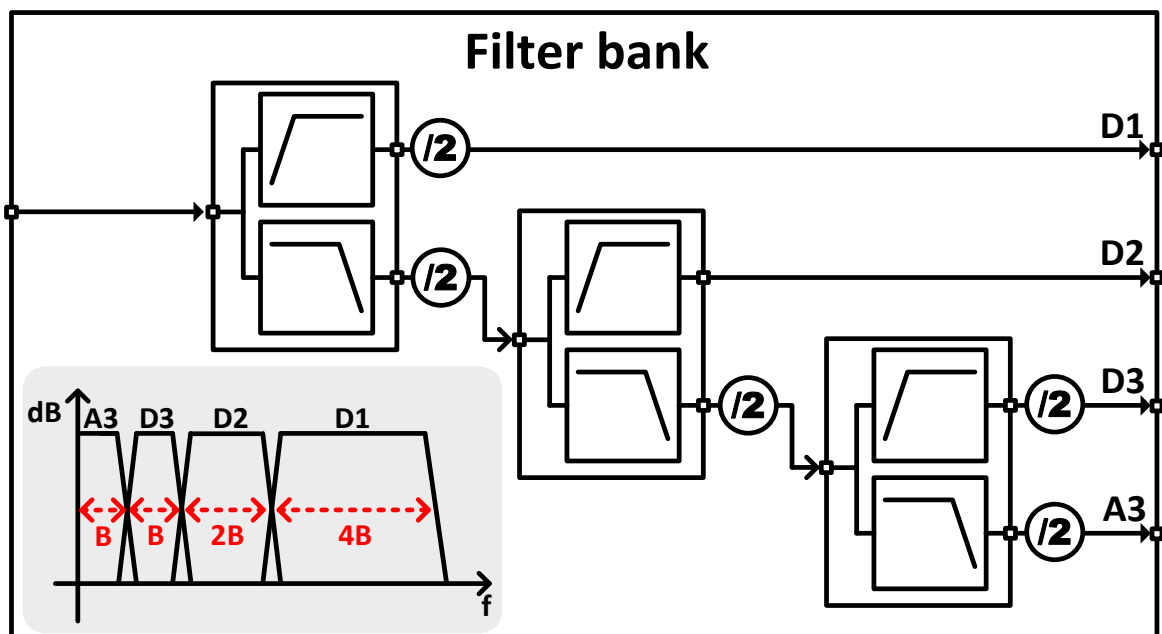
Fig. 13 Block diagram of Filter bank.

Fig. 13 shows block diagram of filter bank in Discrete Wavelet Transform (DWT). It is composed of several stages. Each stage generates *details* by HPF and *approximations* by LPF. The output of each stage is down-sampled by a factor of two then it is passed to the next stage. This process is called multi-resolution analysis. With multi-resolution analysis, scale factor s in Equation (1.1) can be realized in circuit diagram. The results of multi-resolution analysis are coefficients that are details and approximations. They give information of the input signal and are converted into a frequency domain respectively through a Fourier transform. Since the sampling period of each coefficient is different each other, it can say that wavelet transform is performed. The proposed analog circuit for the wavelet transform used in this paper will be explained in section 3.2.2.

Chapter 3

Proposed Wavelet based EMG sensing interface

This chapter describes the proposed EMG sensing interface with basic theory of wavelet transform. The proposed EMG sensing interface includes front-end amplifiers that have additional circuit for eliminating a noise and motion artifact, wavelet filters that decompose the input signal for wavelet transform, and MCU for wireless communication.

3.1 Limitation and Idea for sensing EMG

Bio signal must be sensed through electrode that has inherent limitation. The limitation that is called motion artifact caused by physical movements during the sensing. The motion artifact is dominant constraint that reduces the sensing quality since the physical movements cause the unstable contact of the electrode on the human skin. Unstable contact varies an impedance of electrode then the motion artifact affects the transient signal. However, it is not easy to eliminate motion artifact because the frequency range of motion artifact is similar with that of the bio signal [10].

The proposed idea is the filters based on wavelet transform. The advantages of wavelet transform are as follows; wavelet transform gives frequency information in time domain, and it can analyze the signal by zooming the specific frequency range [8]. Unlike Fourier transform, Wavelet transform has time information and frequency information. This feature makes wavelet transform suitable for real-time monitoring and analysis. With the second advantage, wavelet transform concentrates a meaningful frequency range of bio signal.

This paper suggests wavelet-based EMG sensing system that consists of several front-end amplifiers, wavelet filters and 12bit SAR-ADC. Front-end amplifier and wavelet filters will be explained in section 3.1.1 and 3.1.2 respectively.

3.2 Implementation of integrated circuit
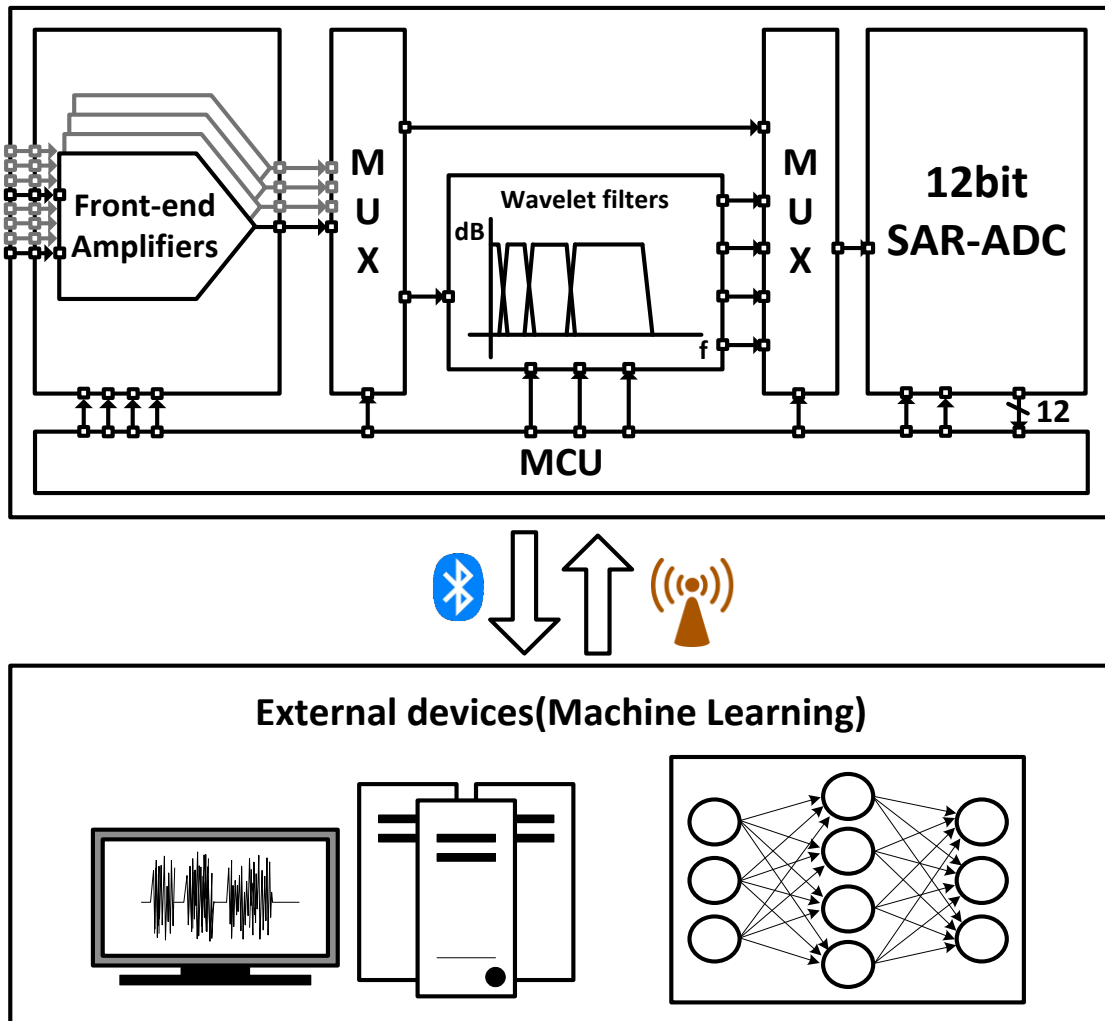
Fig. 14 Overall system of proposed EMG sensing interface.

Fig. 14 shows block the diagram of the proposed EMG sensing interface. It consists of multiple number of front-end amplifiers, wavelet filters, 12bit SAR-ADC and MCU. Multiple number of front-end amplifiers are connected to the first multiplexer (MUX) then it is possible that the MCU can determine the front-end amplifier that is connected to the input of wavelet filters or the input of 12bit SAR-ADC directly. The first MUX also allows the results of amplifiers to be passed to the filter or 12bit SAR-ADC simultaneously by control of MCU. Second MUX determine the connection between wavelet filters and 12bit SAR-ADC. Since the wavelet filters decompose the input signal, its outputs have different frequency range and voltage gain. These decomposed outputs have tolerance to noise because it can eliminate a noise in a certain range of frequency. 12bit SAR-ADC converts the analog

16

input signal to digital data then transmits it with MCU and wireless communication (Bluetooth). The transmitted data is processed in external device. The data process that is operated in an external device will be explained in section 3.2.

3.2.1 Front-end Amplifiers

The front-end amplifier in Fig. 14 consists of CCIA and PGA. After the CCIA, Programmable Gain Amplifier (PGA) amplifies the output of CCIA and implements as a LPF. In this section, the structure of CCIA and additional circuit for eliminating noise from various sources will be explained.
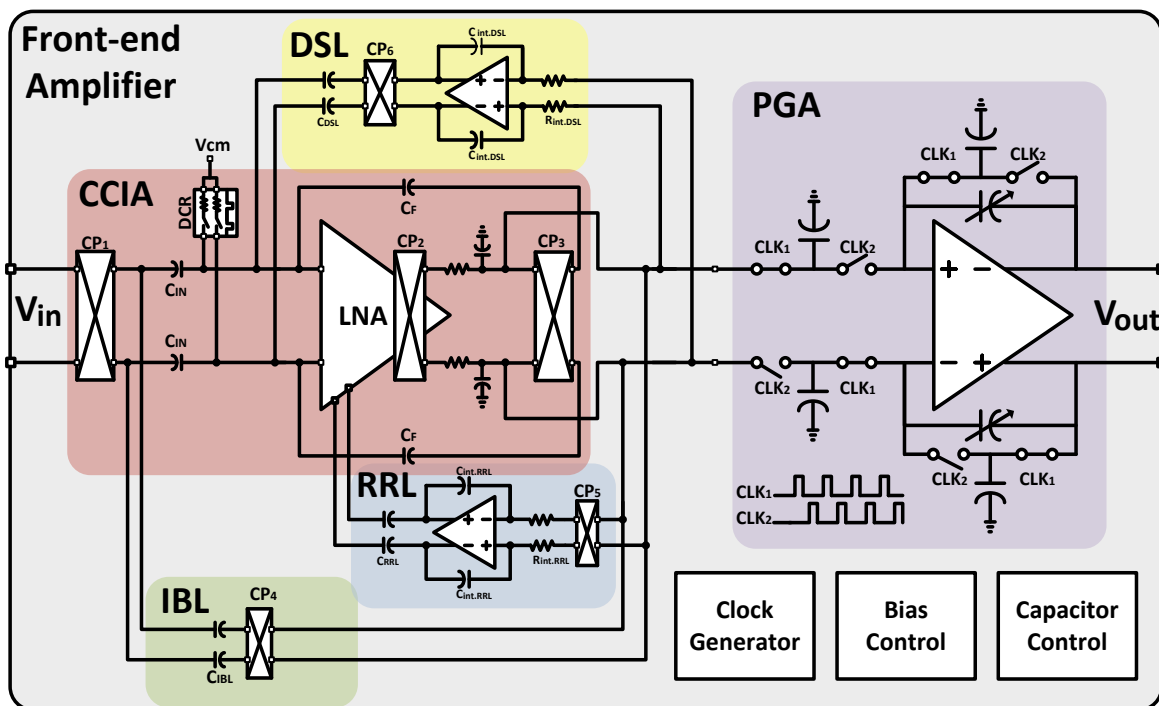
Fig. 15 Proposed front-end Amplifier.

Fig. 15 shows the circuit diagram of proposed front-end amplifiers. The proposed front-end Amplifiers have CCIA structure that consists of Noise Amplifier(LNA), chopper, DC Servo Loop(DSL), Ripple Reduction Loop(RRL), Impedance Boosting Loop(IBL). Unlike the conventional CCIA, the proposed CCIA of front-end amplifier doesn't have resistor at the feedback loop because Programmable Gain Amplifier (PGA) is located after the CCIA then additional LPF is not needed in CCIA. Instead of feedback capacitor, Duty Cycle Resister(DCR) is added to give a common mode voltage at the input of LNA. DCR increases the equivalent resistance by using switch with low duty ratio.

Fig. 16 Duty Cycle Resistor.

DCR is shown in Fig. 16. The equivalent resistance can be expressed as Equation 3.1.

$$R_{eq} \approx \frac{R}{D} = \frac{R}{T_{on} \cdot f_{sw}} \tag{3.1}$$

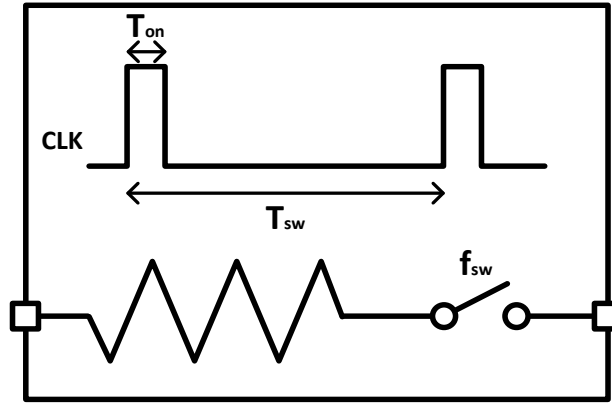The equivalent resistance is very large then almost zero current flows to common mode voltage source. It means common mode voltage can be maintained without voltage drop.

Since the EMG has the amplitude less than 1mV, the EMG signal is susceptible to noise from various noise source. First, input referred noise and 1/f noise from LNA and amplifiers are removed by chopper stabilization. As mentioned in section 2.1.1, input signal is modulated and demodulated by chopper. However, input referred noise and 1/f noise are only modulated from DC to high frequency then is removed by low pass filter. The chopper is an efficient technique for noise reduction. But it decreases input impedance of CCIA. The chopper switches the input capacitors then input impedance is inversely proportional to chopping frequency. Then IBL is needed to boost input impedance of CCIA. The IBL consists of positive feedback capacitor between input and output of CCIA. The feedback capacitor makes the input current small then equivalent input impedance becomes larger. Equation 3.2 – 3.4 show how to decrease the input current by positive feedback capacitor.

$$i_{in} = i_{in.CCIA} - i_{fb} \tag{3.2}$$

$$i_{fb} = sC_{IBL}(V_{out} - V_{in}) \tag{3.3}$$

$$z_{in} = \frac{V_{in}}{i_{in}} = \frac{V_{in}}{i_{in.CCIA} - sC_{IBL}(V_{out} - V_{in})} \tag{3.4}$$

18

The larger the feedback capacitor, the larger feedback current then smaller input current. The small input current increases the input impedance. The chopper (CP4) before the C_{IBL} modulates the output of CCIA to negatively feedback to after the input chopper (CP1).

Chopper has one more trade-off that is a ripple. The input transistor mismatch in CCIA results the offset and this offset becomes a ripple at the output of CCIA by the chopper (CP2). when the input signal is demodulated at the output chopper (CP2), the offset is modulated to high frequency then it can be seen a ripple. It is impossible to make a proper conversion at the 12bit SAR-ADC unless the ripple is removed. The proposed CCIA structure has a ripple reduction loop that is connected to LNA. Compared to the RRL in section 2.1.3, the output of integrator in RRL is modulated and negatively fed back to input node before the first chopper (CP1) that demodulates the offset. However, the proposed structure just negatively fed back to input of LNA then it doesn't need the second chopper in RRL. As mentioned in section 2.1.3, proposed RRL integrates demodulated the ripple then negatively fed back to the input of LNA. As a result, the ripple is reduced.

The proposed front-end amplifier has DC servo Loop that is same as DSL in section 3.1.2. The difference between proposed DSL and explained DSL is the structure of CCIA. The proposed CCIA doesn't have resistor in the feedback loop. The resistor (R_f) in Fig.11 makes a pole then its transfer function is shown in Equation (2.1). However, the transfer function of proposed CCIA without DSL is just a ratio of input capacitor (C_{in}) and feedback capacitor (C_f). To eliminate a DC offset, the proposed DSL makes a pole then makes its transfer function like Equation (3.5):

$$H(s) = \frac{-sR_iC_i \cdot C_{in}}{C_{DSL}+sR_iC_i \cdot C_f} \tag{3.5}$$

The transfer function of proposed CCIA with DSL has one pole on the frequency of $C_{DSL}/R_i \cdot C_i \cdot C_f$. The DC offset from electrodes on the skin of a subject is eliminated by high pass filter.

The proposed front-end amplifier can remove the noise from various sources using the additional circuit above. It is designed to sense various bio signals as well as EMG by adjusting the gain of PGA. The gain, cutoff frequency of PGA and bias current of all the amplifiers are controlled by Microcontroller (MCU).

3.2.2 Wavelet Filters

The most critical noise is motion artifact. As mentioned earlier in this section, motion artifact must be eliminated to improve monitoring and analysis quality. To eliminate the motion artifact, this paper adopts wavelet transform for analysis in frequency domain. The operation of Wavelet transform is divided two steps. As mentioned section 2.2.2, the first step of wavelet transform is decomposing the input signal. DWT decomposes the input signal through several stages that consists of HPF and LPF. The result of each stage is down-sampled by a factor of two then is passed to the next stage. The proposed wavelet filters perform decomposition same as a filter bank in DWT, but it uses analog circuits differently than DWT.
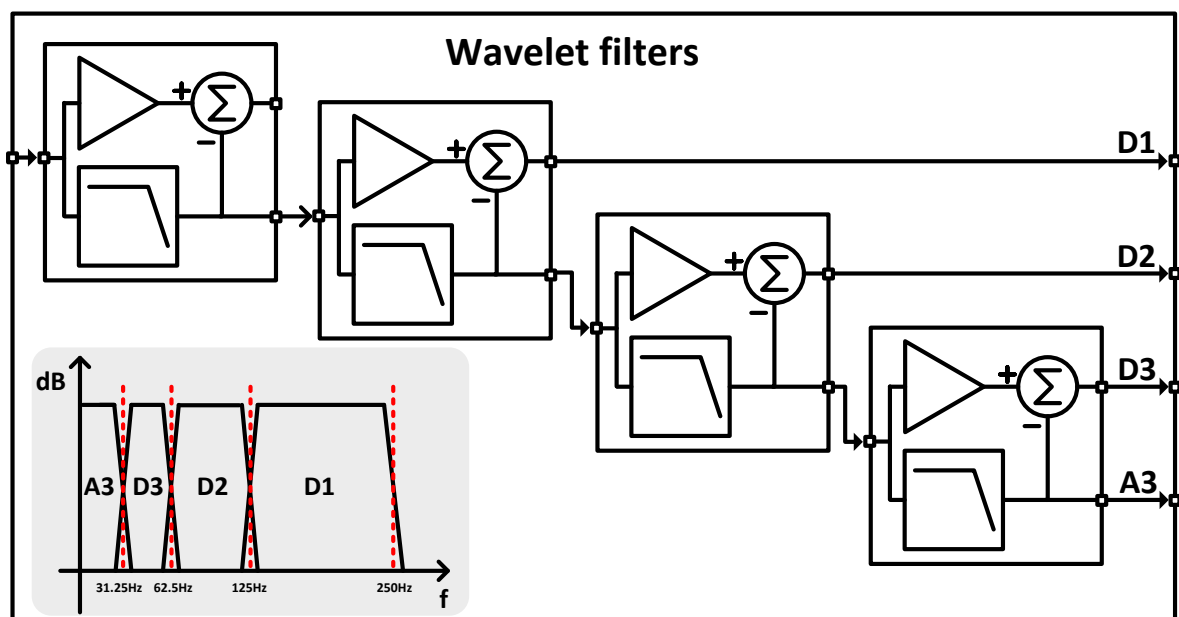

Fig.17 Block diagram of proposed wavelet filters

The main purposes of the proposed wavelet filters are as followed: removing motion artifacts and decomposing input signal in several ranges of frequency. To achieve these goals, the proposed wavelet filters used buffer and subtractor instead of HPF and its block diagram is shown in Fig.17. Because the motion artifact occurs when a subject moves the part of the body with electrode, the signal includes motion artifact in some frequency ranges. The buffered signal is subtracted by low pass filtered signal then the motion artifact that is included in both buffered and filtered signal is removed. Also, when the low frequency component is removed from the primary signal, the subtracted signal can be high pass filtered output because only the high frequency component remains. In conclusion, each stage has been designed to reduce the complexity of a circuit, eliminate noise and allow the role of high pass filter.

In DWT, there are down-samplings in the end of the stages in filter bank. For down-sampling by factor of two, the cut off frequency of each stage in wavelet filters is scaled by a factor of two. This results decomposition of input signal and get analog transient signal which is like coefficients in DWT. The cutoff frequency of each stage is halved from 250Hz for each stage because the power of EMG signal is concentrated in 50 ~ 150 Hz. After the decomposition of wavelet filters, each output is passed to 12bit SAR-ADC to be converted to digital data. The MCU transmits these data to external device (MATLAB in PC) by wireless Bluetooth communication. These data are performed Fourier transform with different sampling period then the frequency information from them is used for machine learning. This paper experiments with the movement of fingers and finally succeeds the monitoring of movement of fingers in real-time.

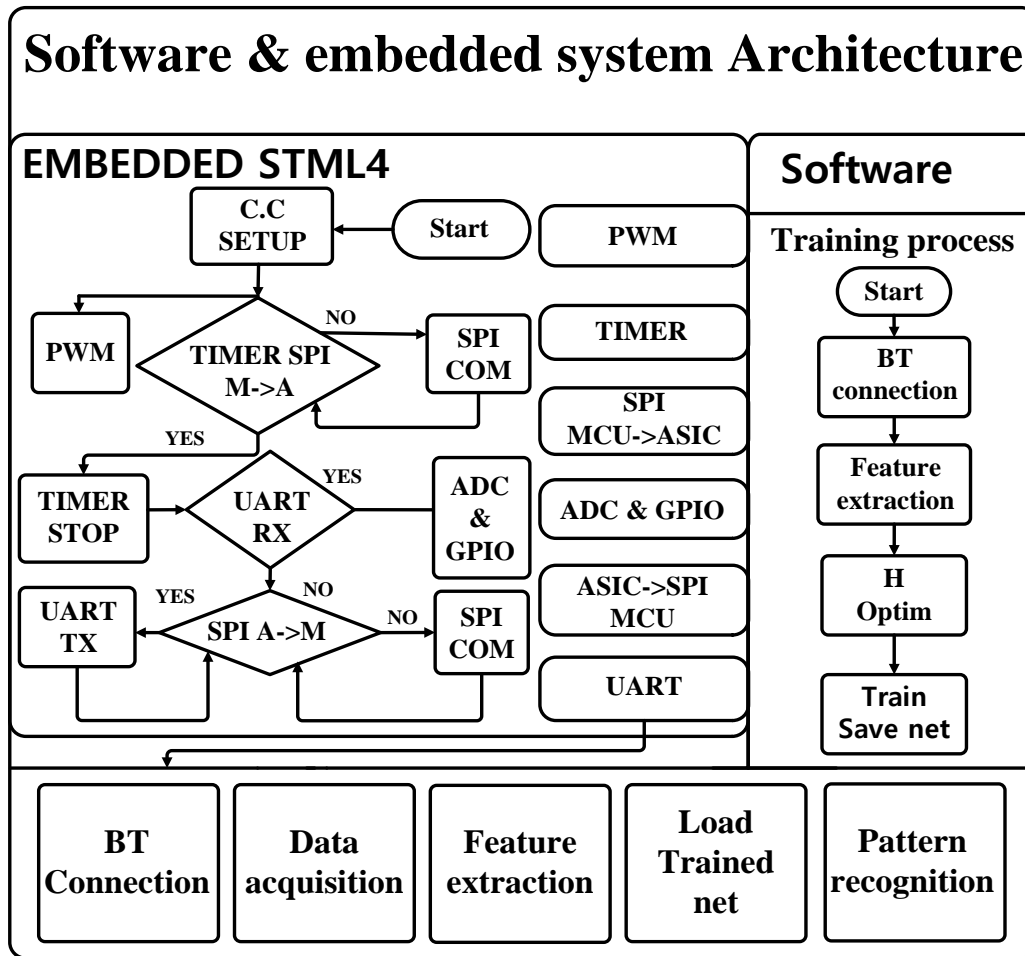## 3.2.3 Machine learning algorithm for EMG recognition

Fig. 18 Machine learning algorithm for finger EMG recognition.

Fig. 18 shows the machine learning algorithm for the recognition of finger movement. The embedded system to control the entire module is implemented by a low power MCU (STM32L4, STmicroelectronis) and its flow chart and block diagram is shown in Fig. 18. Serial Peripheral Interface (SPI) and Universal asynchronous receiver/transmitter (UART) transmits the output of 12bit SAR-ADC to Bluetooth module then Bluetooth modules transmits the output to PC. After acquisition of data, data are converted to frequency information by FFT. *Details* and *approximations* are processed individually with the appropriate sampling frequency for each. The feature of each finger is extracted by the frequency information. In machine learning, the number of hidden layer must be chosen to optimization of accuracy. As the number of hidden layer increase, the motion artifact is also fitted then it causes an overfitting issue. To avoid this issue, the optimization is performed after the feature extraction with frequency information. As a result, the movement of each finger is recognized with features in frequency domain and optimized number of hidden layer.

Chapter 4

Fabrication and measurement results
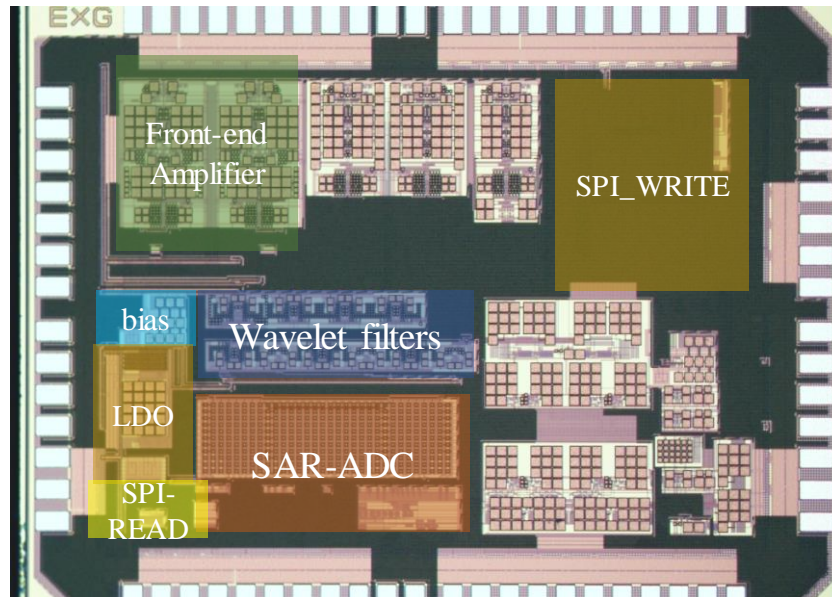
4.1 Fabrication results

Fig. 19 Microphotograph of fabricated chip.

Fig. 19 shows the microphotograph of the fabricated chip. The chip is implemented in CMOS 0.18 μm process and the area of the chip is 2mm × 2mm. The main blocks used in this paper are colored in Fig. 30. The other parts are for the other paper because the 12bit SAR-ADC is shared with EEG analysis circuit.

	This work	TBCAS [16]	TCASⅡ [15]	BioCAS [14]
Year	2018	2015	2017	2017
Process	0.18μ	X	X	X
Application	EMG	EMG	EMG	EMG
Supply [V]	1.8/3.3	3.3	3.7	3.7
Power Consumption w/o communication[mW]	2mW	15mW	6.6mW	X
Total Power consumption[mW]	20mW	36.4mW	100.6mW	44mW
# of electrode channel	2	4 - 8	4	2
# of gestures	5	4 - 7	10	16
Gesture set	Finger	Hand gesture	Trackpad	Finger/ Trackpad
Gesture state	Transient	Steady (hold 3s)	Transient	Steady/ Transient
Recognition Algo.	ANN	SVM	ANN	Deep Forest
Algo. implement	Embedded	Embedded	Embedded	Computer
Accuracy	86%	90%	94%	96%

Table. 1. Comparison table

Table. 1 shows the specification results of fabricated chips and comparison table. The most important feature in this paper is power consumption. Unlike this paper designed the system with a system, other papers purchase and use ASIC (Application-Specific Integrated Circuit) from a company. This paper designs analog front-end amplifiers, wavelet filters and ADC in one chip. The power consumption of the chip without communication module is only 2mW that is much smaller than the Front-end amplifier modules in [14, [15] and [16]. The MCU (STM32L4, STmicroelectronics) is used to control the options inside the chip and read the data from the chip. Then Bluetooth module (HC-06, OEM) transmits the data to external device such as PC with wireless communication. The power consumption of the MCU and Bluetooth module are 17mW and 27mW respectively.

4.2 Measurement results
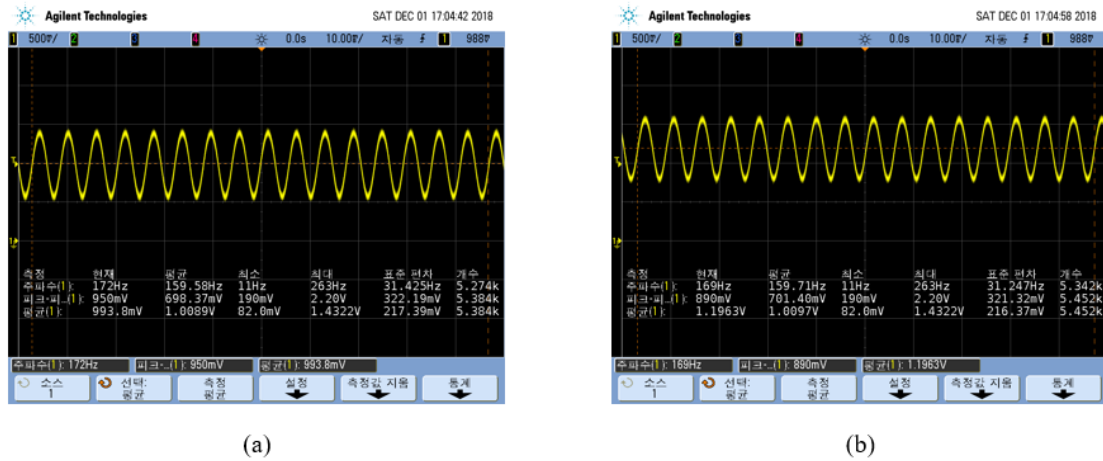
4.2.1 DSL

(a) (b)

Fig. 20 Measurement of DSL with input signal with 10mVpp in 170Hz.
(a) DSL off with no offset, (b) DSL off with 10mV offset

The Fig. 20 shows the performance when the DSL is off. The result of CCIA is shown in Fig. 20(a) when the input signal is sine wave with 170Hz, 10mVpp, and 0.9V common mode voltage. When the offset between differential input is added, the difference of common mode voltage is shown in Fig. 20(b). The common mode voltage increases 0.2V when the 10mV offset is added in differential input.
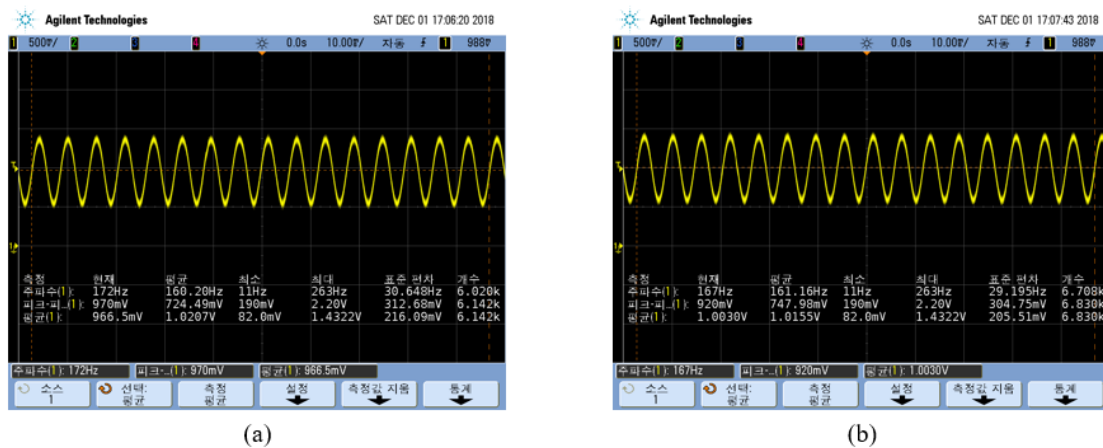

(a) (b)

Fig. 21 Measurement of DSL with input signal that is 10mVpp and 170Hz.
(a) DSL on with no offset, (b) DSL on with 10mV offset

The Fig. 21 shows the performance when the DSL is on. The result of CCIA when the input signal is sine wave with 170Hz, 10mVpp, 0.9V common mode voltage and no offset voltage is shown in Fig.

21(a). Fig. 21(b) shows the result of CCIA with offset voltage in the same way as before. The difference of common mode voltage between them is 40mV. The difference of common mode voltage decreases when the DSL is on with same input signal.

4.2.2 RRL

(a) RRL off

(b) RRL on

(c) RRL off
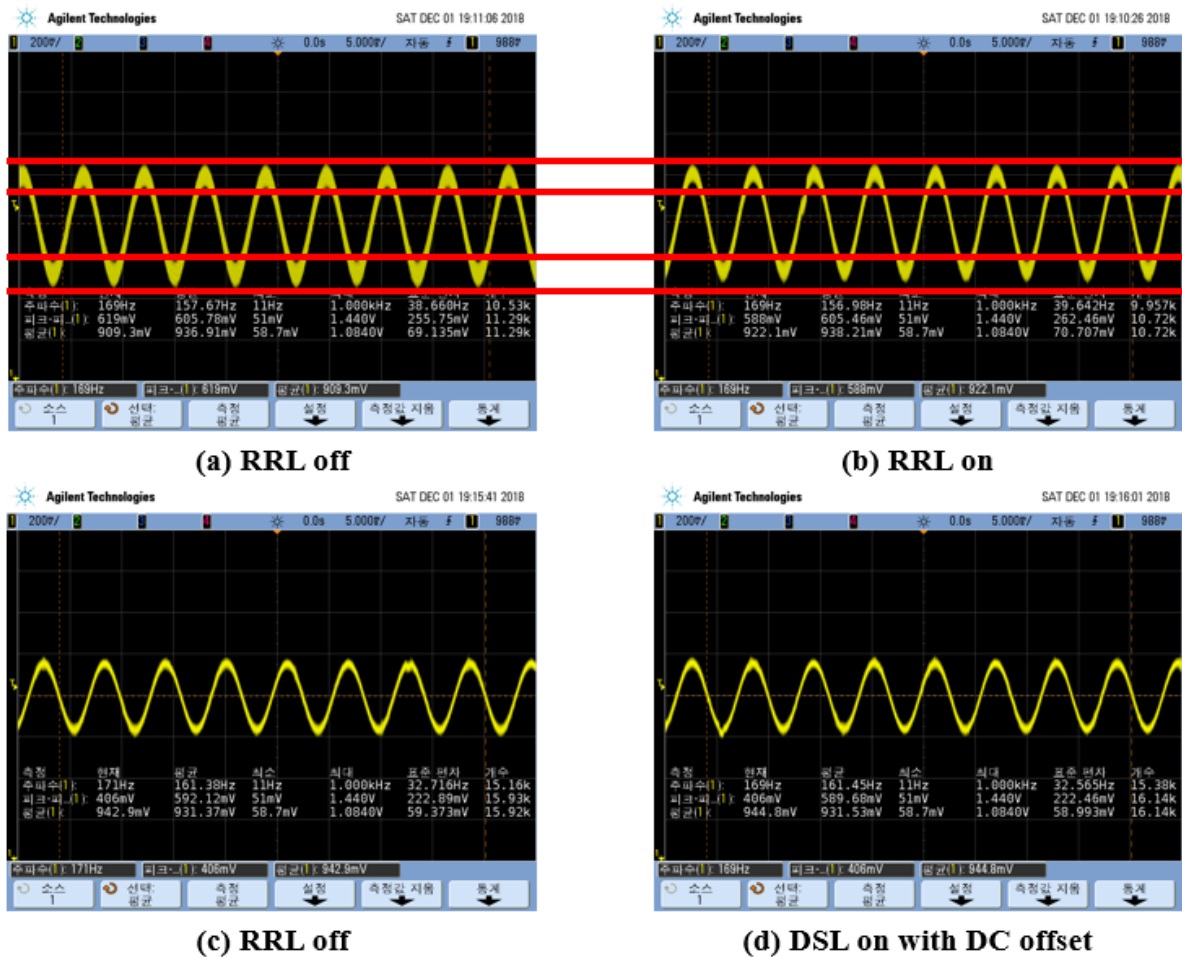
(d) DSL on with DC offset

Fig. 22 Measurement of RRL with input signal that is 5mVpp and 170Hz.
(a) RRL off and (b) RRL on with 75KHz chopper frequency.
(c) RRL off and (d) RRL on with 300KHz chopper frequency.

Fig. 22 shows the measurement of RRL. As mentioned in section 2.1.3, the ripple is induced by chopper and the RRL mitigates the effects of ripple. when the chopper frequency is low, the ripple becomes bigger because the slower the chopper frequency, the larger the difference in the input voltage with the clock. In this experiment, the chopper frequency is 75KHz and 300KHz. The ripple in the Fig. 22 (a) is larger than the ripple in Fig 22. (c). Thus, the chopper frequency must be large value for the EMG sensing. Fig. 22 (a) shows the result of CCIA when RRL is off. The ripple is larger

than the ripple in Fig. 22(b) when the RRL is on. As compared between Fig. 22 (a) and (b), the ripple is mitigated by RRL.
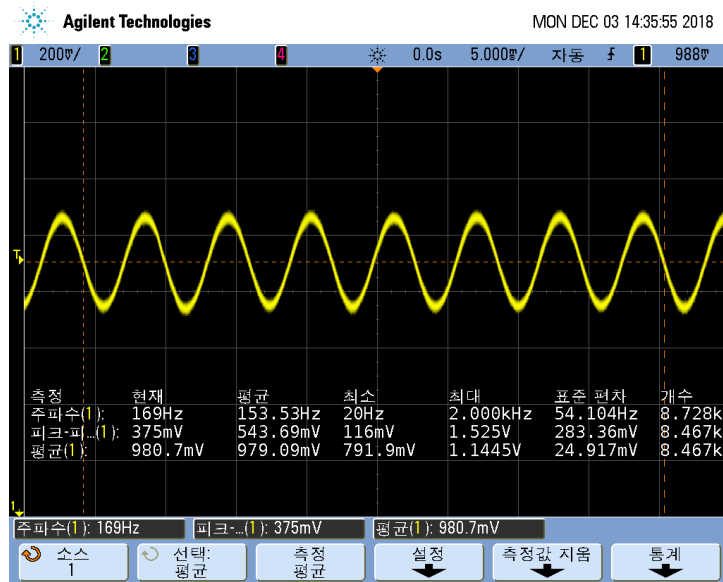

Fig. 23 Measurement of PGA with input signal that is 1mVpp and 250Hz

Fig. 23 shows the result of PGA with input signal that is 1mVpp and 250Hz. The gain of PGA is controlled by MCU in 8 levels. The cap array used for the sensing capacitor is controlled by 3-bit binary code. The gain whose code is 100 is almost 52dB. The maximum gain that is designed is 66dB.
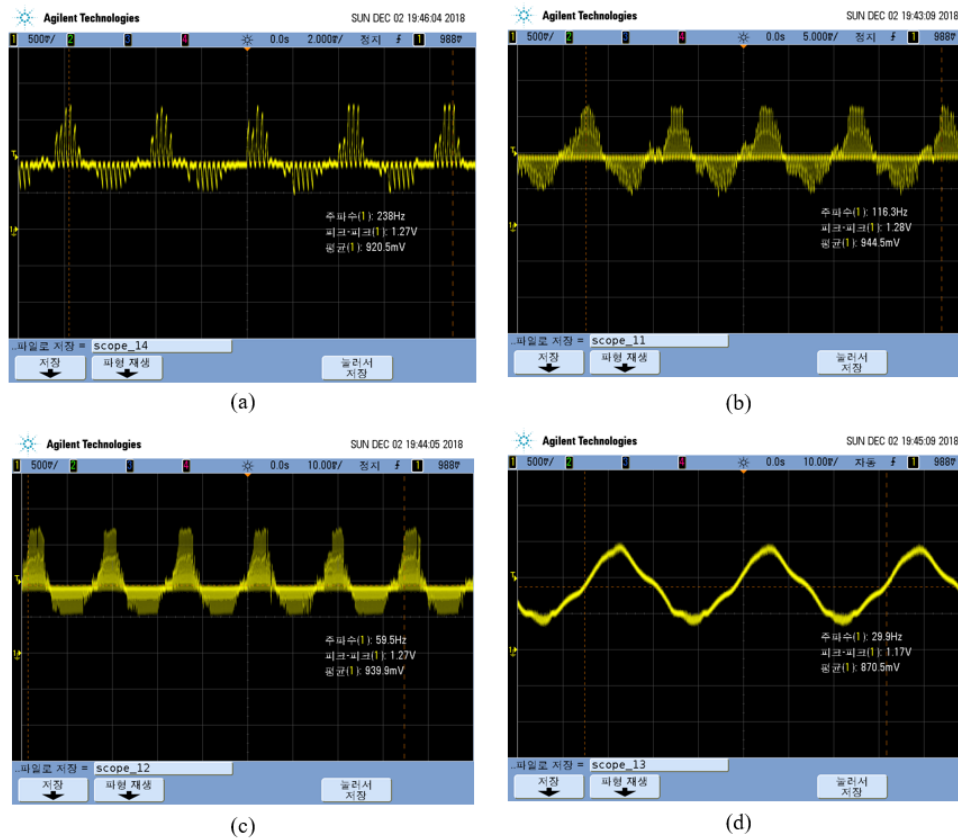
4.2.3 Wavelet Filters

Fig. 24 Measurement wavelet filters.
(a) D1 (b) D2 (c) D3 (d) A3.

   The main purpose of wavelet filters is decomposing the input signal. Fig. 24 shows the result of wavelet filter. The frequency range of each stage are 240 ~ 120Hz, 120 ~ 60Hz, 60 ~ 30Hz, and 30 ~ 0Hz. Then the amplitude of output voltage of each stage is larger in the frequency range of the stage then others. As mentioned in section 3.2, the subtractor is followed then make the HPF then the output of subtractor is *detail*. The subtractor has a switch capacitor structure then it has a reset phase that the output voltage of subtractor is zero. The results shown in Fig. 24 are obtained through the experiment whose input signal of each stage is 1mVpp in common and 240Hz, 120Hz, 60Hz and 30 Hz, respectively.
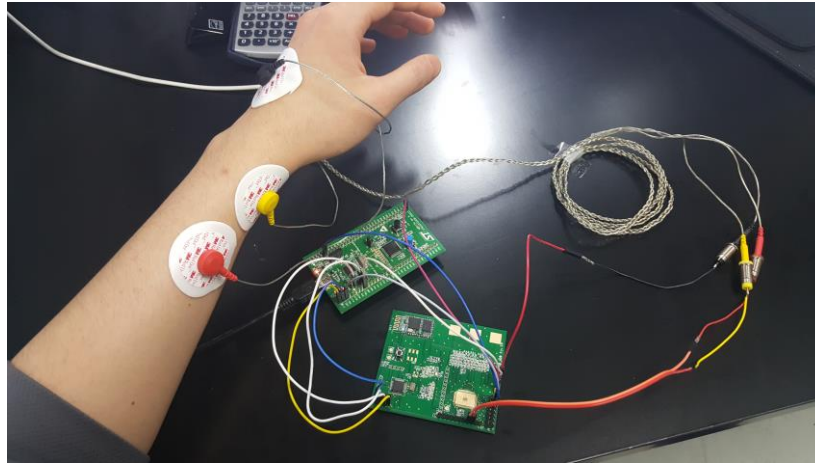
Fig. 25 The EMG sensing system experiment.

Fig. 25 shows the environment of EMG sensing system. To sense the EMG of fingers, the electrodes are attached on the arm. The ground electrode is attached on the back of the hand. The signal from the electrode is amplified by Front-end amplifier then converted to digital data. The output of Front-end amplifier can be processed through analog wavelet filters. The data from the chip is transmitted to PC with Bluetooth module (HC-06, OEM).
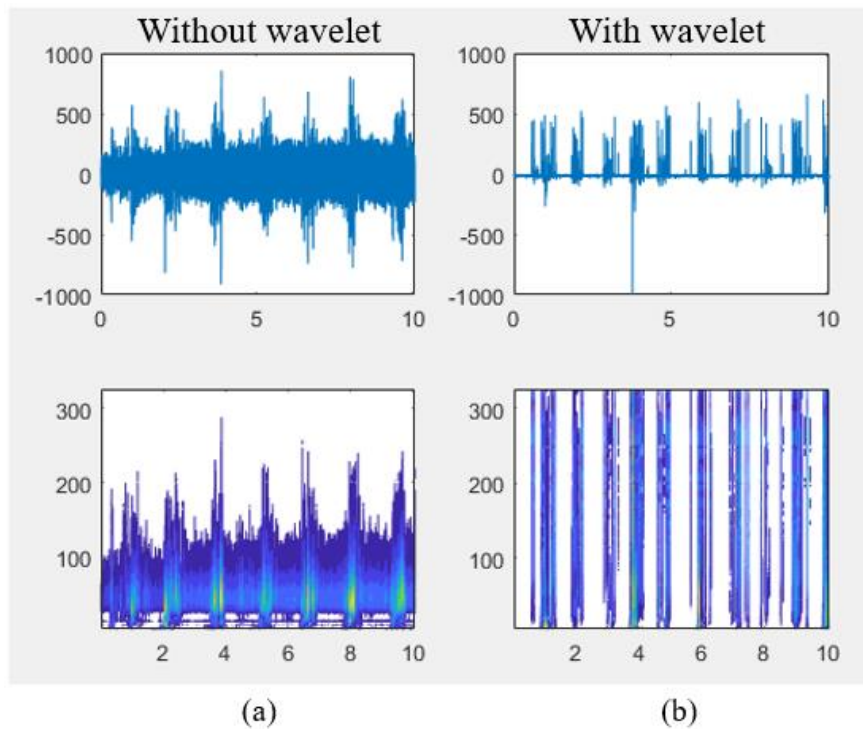

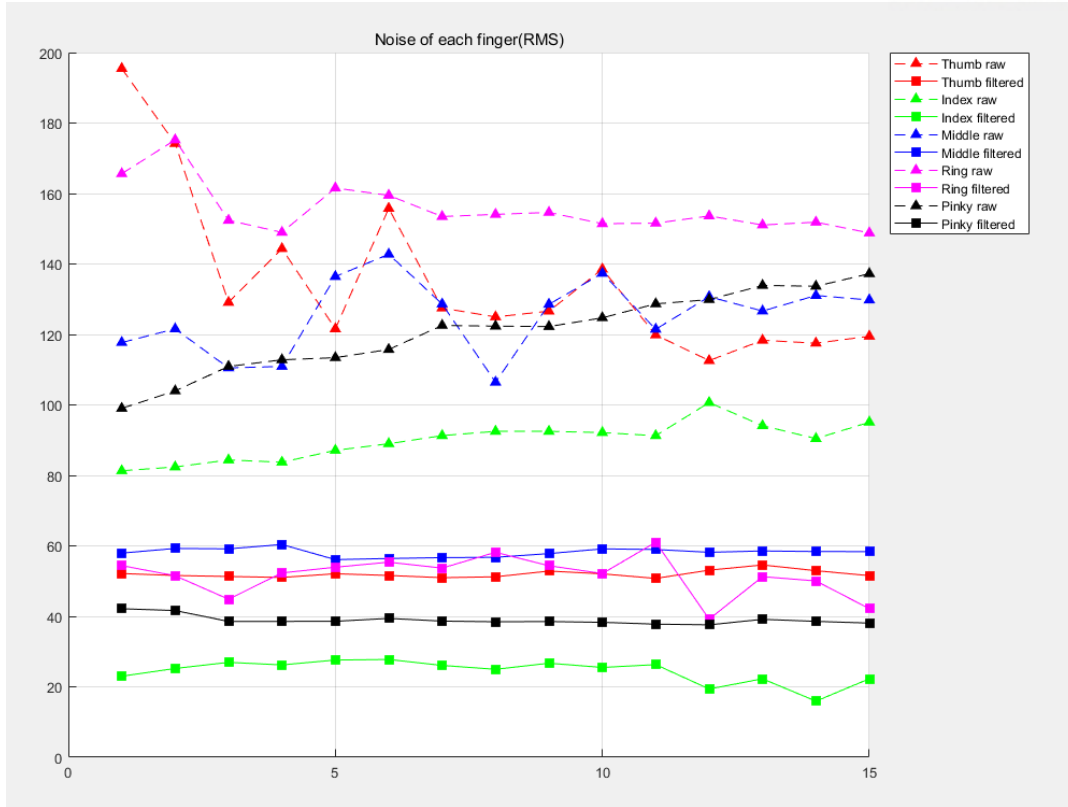Fig. 26 The transmitted data and CWT of the data.

Fig. 27 Graph of the noise of each finger (RMS)

The transmitted data is saved in the PC and processed in MATLAB. Fig. 26 shows the transmitted data and CWT of them. CWT is performed by MATLAB cwt command. As shown in Fig. 26 (a), the EMG from the electrode have lots of noise. The noise can be also converted to digital data and it disturbs the recognition of finger movement. However, the wavelet filtered data in Fig. 26 (b) has less noise then the data in Fig. 26 (a). The wavelet filtered data has high frequency component because of the reset phase in subtractor.

Fig. 27 shows the root mean square value of noise of each finger. The level of noise varies depending on each finger. The y-axis means the RMS value of the digitized data from ADC (-2048 ~ 2048). The level of noise with wavelet filter is smaller than the level of noise without wavelet filter. It means the wavelet filter removes a motion artifact and noise effectively.

To verify the performance of wavelet filters, these data is processed by Machine learning. As mentioned in section 3.3, optimization is performed with 80 data for each finger with 5000 samples per data. 400 data for wavelet filtered and 400 data for raw data that has only front-end amplifier gone through. The result of optimization is shown in Fig. 28
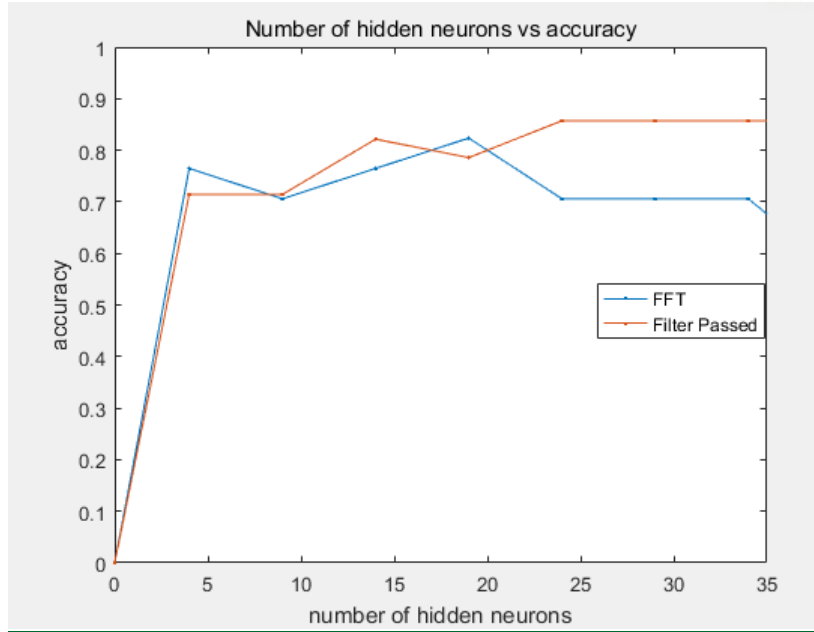
Fig. 28 The optimization result of number of hidden layer.
Blue: Without wavelet filters, Rad: with wavelet filters

The Blue line is raw data without wavelet filters and the rad one is filtered data with wavelet filters.

Because of the above graph, this paper chose the number of hidden layer as 25.
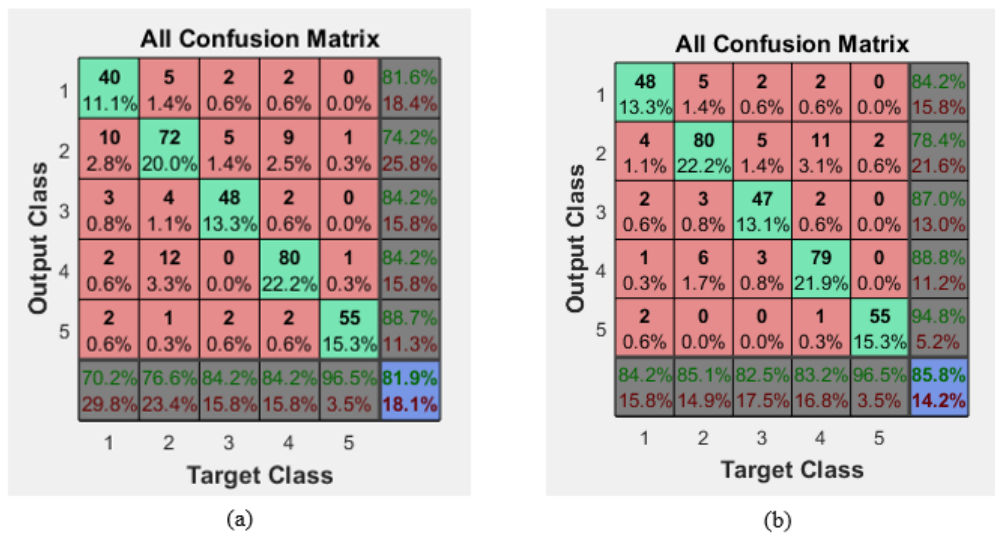
Fig. 29 The confusion matrixes of the finger movement.
(a) Without wavelet filters, (b) with wavelet filters

Fig. 29 shows the confusion matrixes of this paper. 1 to 5 on the x-axis and y-axis means the pinky finger from the thumb. After the feature extraction, based on each feature, it was determined whether any data was expressed as a group of its own. The green colored element means the correct recognition and red one means wrong. For example, when the thumb data are received as target, the

first column shows how the output is distributed. The percentage of each element shows the ratio of the number of the element and the total number of all elements. The green lettering of the gray colored element means the accuracy of each row and column. The total accuracy of the all elements is in the blue colored elements. Fig. 29 (a) shows the confusion matrix whose input data aren't passed through wavelet filters and Fig. 29 (b) shows the confusion matrix whose input data are passed through wavelet filters. The accuracy is 81.9% and 85.8%, respectively. The data passed through wavelet filter have better accuracy than non-filtered data.

Chapter 5

Conclusion

The main targets of this thesis are eliminating a motion artifact and analyzing MG using machine learning based on wavelet transform. To eliminate noise from various source, the proposed front-end amplifier has chopper stabilization. However, chopper stabilization causes two issues as a tradeoff. The first issue is a ripple. Since a chopper is performed by switching the positive and negative input voltages, amplitude of the ripple increases as the chopper frequency decreases. To reduce the ripple, addition circuit is proposed in this thesis. The second issue is a reduction of input impedance. The negative feedback capacitor is added to boosting the input impedance. Also, DC servo loop is added in CCIA to mitigate DC offset from the electrode that is attached to the skin of a subject.

This thesis proposes the filters based on wavelet transform to remove a motion artifact. It decomposes the input signal. Its output is converted by 12bit SAR-ADC individually. The digital data is wireless communicated to MATLAB in PC. The digital data is transformed by FFT individually with specific sampling frequency. After the transform, the motion artifact is removed by detecting the most powerful frequency components in several ranges of frequency. The detected components are passed to machine learning algorithm. The features of each movement of finger is taken by machine learning then the real-time monitoring of finger movement can be performed with these features.

The chip is implemented in TSMC 0.18 μm process. The maximum gain of front-end amplifier is 66dB and each cutoff frequency of wavelet filters is 240Hz, 120Hz, 60Hz and 30Hz. The decomposed signal by the wavelet-based EMG sensing interface is processed individually with the appropriate sampling frequency for each. Those data are converted and analyzed as CWT. With the machine learning, the frequency information of each finger is used to recognize the movement of each finger. The accuracy is 85.8% with wavelet filters and 81.9% without wavelet filters. This result shows the wavelet-based filter is less sensitive to noise and more accurate analysis is possible in frequency analysis with the filter.

References

[1] https://en.wikipedia.org/wiki/Fourth_Industrial_Revolution

[2] Adolfo Benedito, "Printed electronics allow technological leap in wearable devices," MULTIBRIEFS: EXCLUSIVE, http://exclusive.multibriefs.com/content/printed-electronics-allow-technological-leap-in-wearable-devices/science-technology, May, 2017, Web

[3] https://en.wikipedia.org/wiki/Electroencephalography

[4] https://en.wikipedia.org/wiki/Electrooculography

[5] https://en.wikipedia.org/wiki/Electrocardiography

[6] https://en.wikipedia.org/wiki/Photoplethysmogram

[7] https://en.wikipedia.org/wiki/Electromyography

[8] L. Chun-Lin, A Tutorial of the Wavelet Transform., Taipei, Taiwan, 2010

[9] J, Olkkonen, "Discrete wavelet transforms – Theory and applications", 2011

[10] Song, H.; Park, Y.; Kim, H.; Ko, H. Fully Integrated Biopotential Acquisition Analog Front-End IC. Sensors 2015, 15, 25139-25156

[11] Lee, K.; Choi, Y.Y.; Kim, D.J.; Chae, H.Y.; Park, K.; Oh, Y.M.; Woo, S.H.; Kim, J.J. A wireless ExG interface for patch-type ECG holter and EMG-controlled robot hand. Sensors 2017, 17, 1888

[12] Sherman, D. A. (1998). An introduction to wavelets with electrocardiology applications. Herzschrittmachertherapie und Elektrophysiologie, 9(1), 42-52

[13] Park, S.-B., Wilson, J.E., Ismail, M.: 'Peak detectors for multistandard wireless receivers', IEEE Circuits Devices Mag., 2006, 22, (6), pp. 6–9

[14] S. Benatti et al., "A versatile embedded platform for EMG acquisition and gesture recognition," IEEE Trans. Biomed. Circuits Syst., vol. 9, no. 5, pp. 620–630, Oct. 2015.

[15] Zhao, J., Mao, J., Wang, G., Yang, H., & Zhao, B. (2017, October). A miniaturized wearable wireless hand gesture recognition system employing deep-forest classifier. In Biomedical Circuits and Systems Conference (BioCAS), 2017 IEEE (pp. 1-4). IEEE.

[16] Liu, X., Sacks, J., Zhang, M., Richardson, A. G., Lucas, T. H., & Van der Spiegel, J. (2017). The virtual trackpad: An electromyography-based, wireless, real-time, low-power, embedded hand-gesture-recognition system using an event-driven artificial neural network. IEEE Trans. Circuits Syst. II Express Briefs, 64, 1257-1261

Appendix

Acknowledgements

First of all, I would like to thank the professors, Jae Joon Kim, Yun Sik Lee, and Sung Phil Kim who supervised the thesis with busy schedules.

Thanks to my advisor's consideration, I was able to spend my graduate life in a more pleasant laboratory, CSDL. I will never forget the kindness of Professor Jae Joon Kim who accepted me and taught me. It was a happy and meaningful time for me to learn many things not only academic but also humanity. I am always grateful for your teaching and will grow up to be better.

I would like to thank the member of my laboratory, CSDL: Kyeong Hwan Park, Sung Woo Kim, Su Bin Choi, Kwang Muk Lee, Chan Sam Park, Hee Young Chae, Byung Joo Oh, Myeong Woo Kim, Jun Yeong Yeom, and Jeong Hoon Cho. It was lucky to meet you and would like to say thank you and sorry for the three years of my life with you. In Particular, I want to express more appreciation to Kwang Muk Lee and Hee Young Chae for their great help in writing the thesis. I really thank Chan Sam Park for making the opportunity to meet CSDL and I wish your happiness my friend.

During two years of the master's course in CSDL, I felt that I should not forget to thank the people around me. I want to say thank everyone who supported me. Lastly, I really thank my parents for giving me birth and raising me. My everything is made of your effort and sacrifice. Thank you.